Experimental Analysis on Influences of Kinesthetic and Visual Sensations in a Human-Machine Cooperative System Considering Machine Dynamics

YAMAMOTO Tomonori*, MATSUO Yoshiki*, and INABA Takeshi**

* Department of Mechanical and Control Engineering, Tokyo Institute of Technology, Tokyo, Japan
(Tel : +81-3-5734-2545; E-mail: {tyama, matsuo}@ctrl.titech.ac.jp)
** Department of Applied Computer Engineering, Tokai University, Kanagawa, Japan
(Tel : +81-463-58-4042; E-mail: inaba@tokai.ac.jp)

Abstract: The authors investigate influences of manipulator dynamics on and roles of kinesthetic sensation and visual sensation in a Human-Machine Cooperative System (HMCS). At first, the general structure and essential transfer functions of HMCSs are described based on the previous work. Then, after showing theoretical treatment of manipulator dynamics, this paper analyzes the influences on HMCSs in two cases: one is the control design focusing on tool dynamics and reaction force transfer function, and the other is that specifies maneuver transfer function and transfer function for object dynamics variation. In addition to conventional experiments only employing kinesthetic sensation, other experiments with both kinesthetic and visual sensations are performed to examine difference in the roles of these sensations and the validity of the design without the visual sensation.

Keywords: human-machine cooperative system, manipulator dynamics, kinesthetic sensation, visual sensation, self-shaping characteristics of a human operator.

1. Introduction

When a human operator performs a physical task such as machining or manipulating an object by directly operating a motion-controlled robotic system, the task configuration can be regarded as a type of manual control systems from the viewpoint of the operator. The authors call such a system a Human-Machine Cooperative System (HMCS). HMCSs are expected to ease tasks which require both skill and power by cooperation between the human operator and the computer-controlled machine. It is important for its design to consider maneuverability for the operator. Figure 1 shows a simple example of HMCSs.

One of the pioneering work on HMCS is *the Extender Project*[1], which amplifies mechanical strength of the human operator. Another study is on *Virtual Tool Dynamics* by Kosuge *et al.*[2]. They have focused on two essential transfer functions of HMCSs. On the other hand, the authors have focused on maneuverability for human operators and suggested that specifying the other two transfer functions of HMCSs is necessary for the maneuverability when the operator continuously manipulates the controlled machine in contact with the object. However, our previous experiments assumed an ideal manipulator with no dynamics and simulated the object by a computer. Moreover, experiments employed only kinesthetic sensation.

First of all, this paper deals with manipulator dynamics and discusses its effects on HMCSs, for example on stability of control systems based on the virtual tool dynamics when an actual object is used. Then, our design method specifying the other two essential closed-loop is examined, and experiments are performed for both methods. In contrast to these experiments employing only kinesthetic sensation, final experiments let operators use both kinesthetic and visual sensations. Experimental results show each role of kinesthetic sensation and visual sensation and the validity of the previous proposed design method.

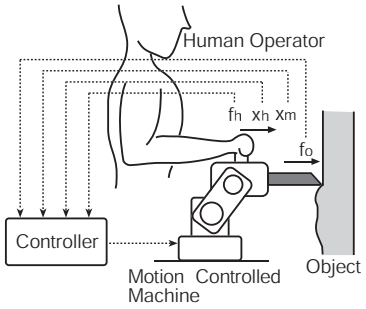

Fig. 1. Simple example of HMCS.

2. General structure considering manipulator dynamics

This section reviews a general structure of all HMCSs stabilizing their tool dynamics and their essential transfer functions, and describes manipulator dynamics used in the study.

2.1. Essential transfer functions for HMCSs

A structure of control systems for HMCSs is illustrated as Fig.2[3], [5]. The system of Fig.2 can be depicted as Fig.3 under the condition that the transfer functions from the operational force $f_h(t)$ and the reaction force $f_o(t)$ to the velocity of the operational point $x_m(t)$ are stable, when the machine is apart from the object $P_O(s)$. Here, $N(s)$ denotes a left coprime factor on RH_∞ (RH_∞ denotes the set of stable and proper transfer function matrices), and two compensators, $K_H(s)$ and $K_O(s)$, should be included in RH_∞. Then, four essential transfer functions are expressed[4], [5] by using the sensitivity function of the system in Fig.3 as

$$S_O(s) \triangleq \left(I + N(s)\,K_O(s)\,P_O^{-1}(s)\right)^{-1}. \tag{1}$$

Tool dynamics : the transfer function from the operational force $f_h(t)$ to the motion of the operational point $x_m(t)$ when the machine is apart from the object.

$$G_T(s) = N(s)\,K_H(s) \tag{2}$$

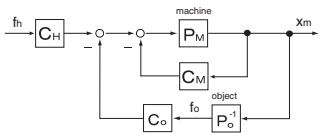

Fig. 2. Configuration of a control system for HMCSs.

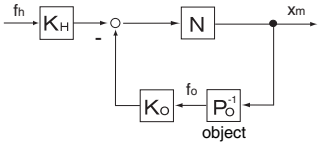

Fig. 3. General structure of all HMCSs with stable tool dynamics.

Reaction force transfer function : the transfer function from $f_o(t)$ to $f_h(t)$ when $x_m(t)$ is fully constrained.

$$G_F(s) = K_H^{-1}(s)\, K_O(s) \tag{3}$$

Maneuver transfer function : the transfer function from $f_h(t)$ to $x_m(t)$ when the machine contacts and moves with the object.

$$G(s) = S_O(s)\, N(s)\, K_H(s) \tag{4}$$

Transfer function for object dynamics variation : this function represents how variation of the object impedance $P_O^{-1}(s)$ affects the maneuver impedance $G^{-1}(s)$ from the viewpoint of the human operator.

$$G_\Delta(s) = I - S_O(s) \tag{5}$$

A condition that $S_O(s)$, $K_H(s)$ and $K_O(s) \in RH_\infty$ restricts feasible classes of $G(s)$ and $G_\Delta(s)$. Since the general structure has two design freedom with $K_H(s)$ and $K_O(s)$, two transfer functions can be chosen in order to specify the control system design. While section 3. focuses on $G_T(s)$ and $G_F(s)$, sections 4. and 5. specify $G(s)$ and $G_\Delta(s)$.

2.2. Influences of manipulator dynamics

Generally, a motion controlled manipulator has a certain dynamics, though the previous studies[3], [4], [5] have neglected them for simplicity. An experiment shows that the manipulator used in this study (RV-E4N, Mitsubishi Electric Co.) has the dynamics $R(s)$ approximated by a first-order lag with a time delay. Then, when the system of Fig.3 is implemented with the manipulator, the block diagram is illustrated as Fig.4, where $N(s)$ is chosen as a set of a mass and a damper similarly as conventional studies[2]: $N(s) = \frac{1}{M_T s + D_T}$.

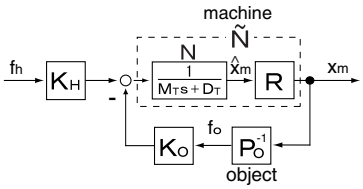

Fig. 4. Block diagram of an HMCS with stable tool dynamics considering the manipulator dynamics.

Then, the influence of $R(s)$ on equations (2), (4), (5), and Fig.3 is dealt with by replacing $N(s)$ with $\tilde{N}(s)$ as follows:

$$N(s) \;\rightarrow\; \tilde{N}(s) \;=\; R(s)\, N(s). \tag{6}$$

In the present paper, the manipulator dynamics $R(s)$ is approximated as equation (7) using a first-order *Padé approximation* for the time delay.

$$R(s) \doteqdot \frac{1}{Ts+1}\,\frac{1-\frac{L}{2}s}{1+\frac{L}{2}s} \tag{7}$$

3. HMCS based on the virtual tool dynamics

Kosuge *et al.* have suggested the virtual tool dynamics method, which specifies both the tool dynamics $G_T(s)$ and the reaction force transfer function $G_F(s)$. This section analyzes influences of the manipulator dynamics $R(s)$ on control systems based on this design method.

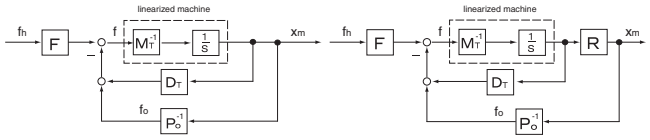

(a) Case A: Using an ideal manipulator.

(b) Case B: Considering the manipulator dynamics.

Fig. 5. Block diagrams for a design based on the virtual tool dynamics.

3.1. Design examples based on the virtual tool dynamics method

Case (A) Using an ideal manipulator[2], [4]

Figure 5 (a) shows a control system using an ideal manipulator with no dynamics. This control system corresponds to the general framework regarding transfer functions in Fig.2 as $P_M(s) = \frac{1}{M_T s}$, $C_M(s) = D_T$, $C_H(s) = F$, and $C_O(s) = 1$. Then, $G_T(s)$ and $G_F(s)$ are obtained as:

$$G_T(s) = \frac{F}{M_T s + D_T}, \quad G_F(s) = F^{-1}. \tag{8}$$

Case (B) Including the manipulator dynamics

From equation (6), a control system based on the virtual tool dynamics including the manipulator dynamics is shown in Fig.5 (b), so $G_T(s)$ and $G_F(s)$ are expressed as

$$\tilde{G}_T(s) = \frac{1}{Ts+1}\,\frac{1-\frac{L}{2}s}{1+\frac{L}{2}s} G_T(s), \quad G_F(s) = F^{-1}. \tag{9}$$

3.2. Choosing a desirable class of $G_T(s)$

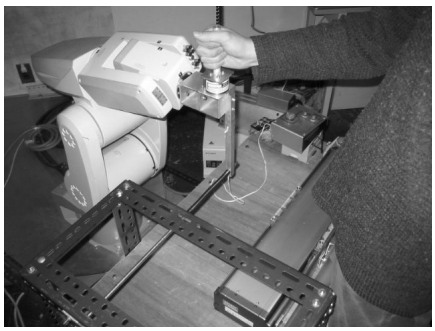

Fig. 6. Scene of an experiment.

In experiments, a subject is instructed to counterbalance the force disturbance $f_d(t)$ applied randomly by a computer,

only by voluntary operation wearing an eye mask. The operation is restricted to a straight-line motion in right and left direction of the operator. Analyzing four signals, f_h, f_d, f_o, and $\hat{x}_m$ recorded on the computer, the maneuver transfer function $G(s)$, the human operational transfer function $H(s)$, and the open-loop transfer function $G(s)H(s)$ are identified.

The previous studies have noted two important points on a manual control system through similar experiments[3], [5]: there is a relationship between the self-shaping performance of an operator and maneuverability for him/her, and the crossover frequency of open-loop transfer function $G(s)H(s)$ is a good measure for the maneuverability because attaining a high crossover frequency means that the operator can control the machine in a wider bandwidth.

Before experiments using actual springs as the object, a desirable class of the tool dynamics $G_T(s)$ should be specified. Experiments are performed without the object $P_O^{-1}(s)$, so an equivalent control object $G(s)$ is expressed as equation (10) when $F = 1$, from equation (9).

$$\tilde{G}_T(s) = \frac{1}{M_T s + D_T} \frac{1}{Ts+1} \frac{1 - \frac{L}{2}s}{1 + \frac{L}{2}s} \tag{10}$$

Considering equation (10), sets of parameters are prepared as follows:

(i) $\tilde{G}_T(s)$s are dominated by viscosity D_T
(M_T[kg], D_T[Ns/m]) =
(0.33, 33), (0.56, 56), (1.0, 100), (1.8, 180), (3.3, 330)

(ii) $\tilde{G}_T(s)$s are dominated by inertia M_T
(M_T[kg], D_T[Ns/m]) =
(5.6, 0.56), (10, 1.0), (18, 1.8), (33, 3.3), (56, 5.6)

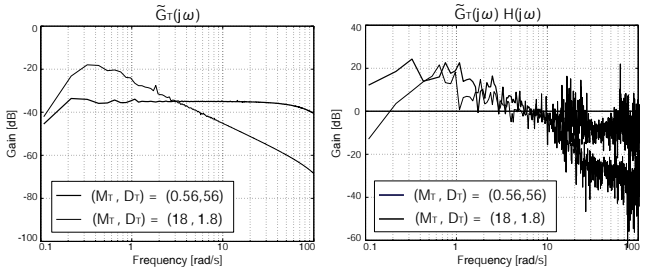

(a) Frequency responses of $\tilde{G}_T(s)$s.

(b) Frequency responses of $\tilde{G}_T(s)H(s)$s for $\tilde{G}_T(s)$s.

Fig. 7. Loop-shaping characteristics of a human operator for two examples of $\tilde{G}_T(s)$s.

From the cases (i) and (ii), the sets of (M_T[kg], D_T[Ns/m]) = (0.56, 56) and (18, 1.8) are chosen respectively because the frequency responses of them meet the conditions for a good maneuverability to the most extent. Then, Figure 7(a) and (b) show frequency responses of $\tilde{G}_T(s)$s and $\tilde{G}_T(s)H(s)$s for $\tilde{G}_T(s)$s, using these parameters. From Fig.7(b), the desirable class of $G_T(s)$ ($M_T = 0.56$[kg], $D_T = 56$[Ns/m]) is obtained because of its higher crossover frequency.

3.3. Experiments using an actual spring as the object based on the virtual tool dynamics

Adopting the parameters from the previous subsection, experiments using actual springs as shown in Table 1 are performed. An experimental setup is as follows: a metal square bar, attached to the manipulator; and strain gauges, stuck on the bar. When an actual spring is compressed by the manipulator, strain of the bar produces some voltage, converted into the reaction force $f_o(t)$. Five actual springs below are prepared for the object of experiments.

Table 1. Elasticity coefficients E_O[N/m] of five springs.

spring1	spring2	spring3	spring4	spring5
200	362	599	925	1855

Case (A) Using an ideal manipulator

To examine influences of the manipulator dynamics clearly, let us assume the case using an ideal manipulator with no dynamics theoretically. When objects are chosen as $P_O^{-1}(s) = \frac{E_O}{s}$, the maneuver transfer function $G(s)$ is expressed as

$$G(s) = \frac{G_T(s)}{1 + G_T(s)\frac{E_O}{s}}, \tag{11}$$

where $F = 1$, from equations (1), (4), and (8).

Case (B) Including the manipulator dynamics

Now, the manipulator dynamics is included in the control system. From Fig.5(b) and equations (1), (4), and (9), the maneuver transfer function is written as

$$\tilde{G}(s) = \frac{\tilde{G}_T(s)}{1 + \tilde{G}_T(s)\frac{E_O}{s}}. \tag{12}$$

Substituting the parameters, M_T and D_T, obtained from section 3.2. and an elasticity coefficient E_O in Table 1, while the case (A) is always stable for five springs, the case (B) becomes unstable when the spring5 is chosen as the object.

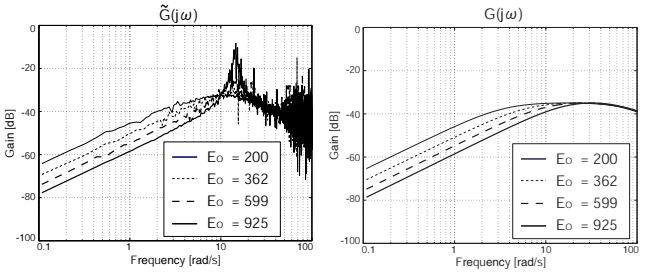

(a) Frequency responses of $\tilde{G}(s)$s, including the dynamics.

(b) Frequency responses of $G(s)$s, the ideal case.

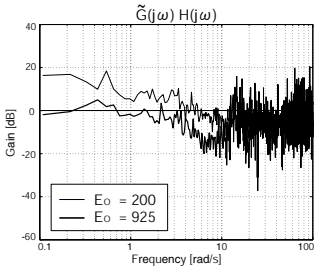

(c) Frequency responses of $\tilde{G}(s)H(s)$s for $\tilde{G}(s)$s.

Fig. 8. Influence of the four springs on the loop-shaping characteristics.

Figure 8(a), (b), and (c) show frequency responses of $\tilde{G}(s)$s, $G(s)$s, and $\tilde{G}(s)H(s)$s. While the data of Fig.8(a) and (c) are taken from the experiments, those of Fig.8(b) are simulated by the computer because such an ideal manipulator does not exist. Comparing Fig.8(a) and (b), the differences between them are shown over about 7[rad/s]. The manipulator dynamics $R(s)$ causes the open-loop gain differences. When spring5 is used as the object, the experiment cannot be completed as expected because $\tilde{G}(s)$ is unstable. Moreover, from Fig.8(c), the bigger the elasticity coefficient of the spring is, the lower both the crossover frequency and the open-loop gain at low frequencies become. As a result, the subject cannot control the machine with the object skillfully as harder springs are selected.

To conclude, the manipulator dynamics $R(s)$ makes differences between frequency responses of $G(s)$ and $\tilde{G}(s)$. The maneuver transfer function $\tilde{G}(s)$ becomes unstable when a stiff spring is used as the object, which is confirmed experimentally.

4. HMCS specifying both $G(s)$ and $G_\Delta(s)$

The authors have proposed a method specifying the maneuver transfer function $G(s)$ and the transfer function for object dynamics variation $G_\Delta(s)$[3], [4], [5]. This section deals with the same experiments performed in the section 3. in order to examine influences of the manipulator dynamics $R(s)$ on control systems based on our method.

4.1. Analysis on design constraints considering the manipulator dynamics

Following the previous work[4], [5], $G(s)$ and $G_\Delta(s)$ should be specified for a good maneuverability. Specifying them and considering the dynamics $R(s)$ give the constraints on the control system. Only spring-type objects are considered, and the machine dynamics $N(s)$ and the nominal value of the object $P_{nm}^{-1}(s)$ are described as

$$N(s) = \frac{1}{M_T s + D_T}, \tag{13}$$

$$P_{nm}^{-1}(s) = \frac{E_{nm}}{s}. \tag{14}$$

Case (A): Using an ideal manipulator[5]

Assuming that a subject operates an ideal manipulator with no time delay, the desirable class of nominal $G(s)$ is chosen as

$$G_D(s) = \frac{s}{M_D s^2 + D_D s + K_D}, \tag{15}$$

which can be realized only when the object is chosen as the nominal model. The transfer function $G_\Delta(s)$ is chosen as a second order low-pass filter,

$$G_\Delta(s) = \frac{\alpha\,\omega_n^2}{s^2 + 2\zeta\omega_n s + \omega_n^2}\,. \tag{16}$$

Then, from equations (1), (4), and (5),

$$\begin{cases} K_H(s) = \frac{(M_T s+D_T)s}{M_D s^2+D_D s+K_D}\,\frac{1}{1-G_\Delta(s)}\,, \\ K_O(s) = \frac{(M_T s+D_T)s}{E_{nm}}\,\frac{G_\Delta(s)}{1-G_\Delta(s)}\,. \end{cases} \tag{17}$$

Using these compensators, the actual maneuver transfer function $G(s)$ is expressed as

$$G(s) = \frac{1}{1+G_\Delta(s)(\frac{E_O-E_{nm}}{E_{nm}})}\,G_D(s) \tag{18}$$

when the object is written as $P_O^{-1}(s) = \frac{E_O}{s}$.

Case (B): Considering the manipulator dynamics

Now, consider the dynamics of the manipulator. The transfer function of the machine is described as

$$\tilde{N}(s) = \frac{1}{Ts+1}\,\frac{1-\frac{L}{2}s}{1+\frac{L}{2}s}\,N(s)\,. \tag{19}$$

In this paper, $G_D(s)$ and $R(s)$ are simply put in series just like $\tilde{N}(s)$ in subsection 2.2. to decide the feasible transfer function $\tilde{G}(s)$:

$$\tilde{G}_D(s) = \frac{1}{Ts+1}\,\frac{1-\frac{L}{2}s}{1+\frac{L}{2}s}\,G_D(s). \tag{20}$$

The transfer function $\tilde{G}_\Delta(s)$ is similarly chosen, referring to equation (16), as

$$\tilde{G}_\Delta(s) = \frac{1}{Ts+1}\,\frac{1-\frac{L}{2}s}{1+\frac{L}{2}s}\,G_\Delta(s)\,. \tag{21}$$

Then, $\tilde{K}_H(s)$ and $\tilde{K}_O(s)$ are obtained.

$$\begin{cases} \tilde{K}_H(s) = \frac{(M_T s+D_T)s}{M_D s^2+D_D s+K_D}\,\frac{1}{1-\tilde{G}_\Delta(s)}\,, \\ \tilde{K}_O(s) = \frac{(M_T s+D_T)s}{E_{nm}}\,\frac{\tilde{G}_\Delta(s)}{1-\tilde{G}_\Delta(s)}\,. \end{cases} \tag{22}$$

Substituting equations (1), (19), (22), and $P_O^{-1}(s) = \frac{E_O}{s}$ into (4) gives the actual maneuver transfer function as

$$\tilde{G}(s) = \frac{1}{1+\tilde{G}_\Delta(s)(\frac{E_O-E_{nm}}{E_{nm}})}\,\tilde{G}_D(s)\,. \tag{23}$$

In conclusion, the stability of equations (17) and (18) in Case (A) depends on the maximum gain of $G_\Delta(s)$ and the difference between the nominal and the actual springs, E_{nm} and E_O; on the other hand in the Case (B), the condition whether equations (22) and (23) are stable depends on the set of parameters of $\tilde{G}_\Delta(s)$ as well as the two requirements in Case (A) because $\tilde{G}_\Delta(s)$ contains the manipulator dynamics $R(s)$. Thus, considering the manipulator dynamics restricts feasible classes of $\tilde{G}_\Delta(s)$ and the objects $P_O(s)$. In the present experiments, $\tilde{G}_\Delta(s)$ can be chosen arbitrarily because the experiments does not require object dynamics variation recognition, so all transfer functions and compensators are stable.

4.2. Parameter settings

The spring1 is chosen as a nominal model (E_{nm} = 200[N/m]). Based on the preliminary experiments[5], the sets of desirable parameters of the machine and the maneuver transfer function for the subject are as follows:

$$\begin{cases} M_T = 0.56\text{[kg]},\ D_T = 56\text{[Ns/m]}, \\ M_D = 0.56\text{[kg]},\ D_D = 56\text{[Nm/s]},\ K_D = 33\text{[N/m]}\,. \end{cases}$$

From a system identification experiment, the dynamics parameters of the manipulator are identified as follows:

$$T = 0.027, \quad L = 0.0385\,[\mathrm{s}]\,.$$

Again, the parameters of $\tilde{G}_\Delta(s)$ is arbitrary because of the simple experiments, so in order to simplify equation (22), they are chosen as

$$\zeta = \frac{D_D}{2\sqrt{K_D M_D}}\,,\ \omega_n = \sqrt{\frac{K_D}{M_D}}\,,\ \alpha = 1\,.$$

4.3. Experimental results and discussions

Although equations (18) and (23) are both stable for springs 1 to 5, spring5 cannot be used as the object owing to the permissible load range of the manipulator; only four springs are used. Figure 9(a), (b), and (c) show the frequency responses of $\tilde{G}(s)$s, $G(s)$s, and $\tilde{G}(s)H(s)$s. By the same token in subsection 3.3. , the frequency responses of $G(s)$s in Fig.9(b) are obtained by a computer simulation.

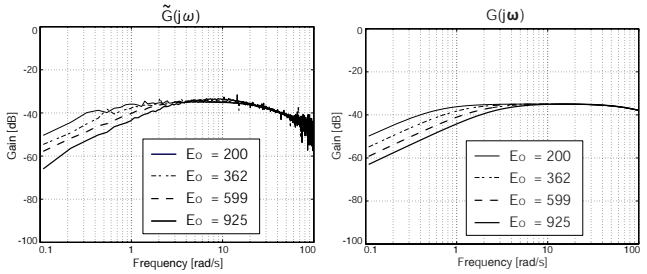

(a) Frequency responses of $\tilde{G}(s)s$, considering the dynamics.

(b) Frequency responses of $G(s)s$, the ideal case.

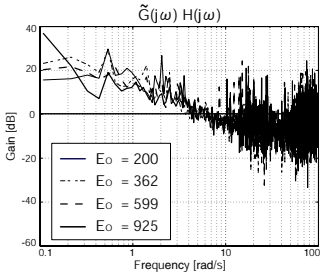

(c) Frequency responses of $\tilde{G}(s)H(s)s$ for $\tilde{G}(s)s$.

Fig. 9. Influence of the four springs on the loop-shaping characteristics.

1. From Fig.9(c), because gain variation in $\tilde{G}(s)$s is small, crossover frequencies are nearly equal, and all $\tilde{G}(s)H(s)$s have gain slope of -20[dB/dec] around the crossover frequency, which implies that the subject can manipulate all of the control objects very well.
2. Comparing Fig.9(a) and (b), the frequency responses of ideal $G(s)$s and $\tilde{G}(s)$s are close at low frequencies; the differences are only shown at high frequencies, i.e. over crossover frequencies. Thus, operating the ideal manipulator would not affect the human maneuverability.

It is clear that despite the constraints of the manipulator dynamics on the stability of control systems, specifying the desirable class of the maneuver transfer function for the operator reduces the differences of the gain due to springs, which enables him to handle more comfortably. Moreover, since the frequency responses of $\tilde{G}(s)$s are almost similar to those of ideal $G(s)$s, the subject could not operate the ideal machine with the object more skillfully.

5. HMCS using both kinesthetic and visual sensations

When a human operator manipulates a machine, it is quite natural to use his/her eyes in operation. Conventional experiments[1]-[5] have employed only kinesthetic sensation, so this section deals with an HMCS using both kinesthetic and visual sensations. First, a block diagram of an HMCS with both sensations is explained. Second, the two types of $G(s)s$ are prepared for experiments based on the previous work[5]. Then, the experiments employing both sensations is performed. By comparing the results with those of section 4, roles of kinesthetic sensation and visual sensation are clarified. Besides, comparison for the two $G(s)$s examines if specifying the desirable class of $G(s)$ is relevant even when both of the sensations are employed.

5.1. Equivalent manual control system of an HMCS using both sensations

In this section, more general class of HMCSs is treated where a subject employs both kinesthetic and visual sensations. This system can be represented by the block diagram in Fig.10.

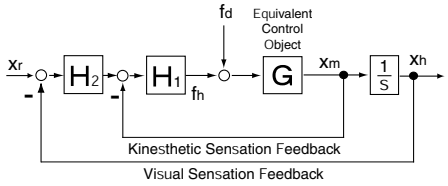

Fig. 10. Block diagram of an HMCS using both kinesthetic and visual sensations.

From Fig.10, human operational transfer function $H(s)$ can be written as

$$H(s) = H_1(s)\left(1 + \frac{H_2(s)}{s}\right)\,, \tag{24}$$

when the system is described as a single feedback system choosing the velocity $x_m(t)$ of the operational point as the controlled output. In this system, $H(s)$ consists not only of the kinesthetic compensating transfer function $H_1(s)$ but also of the visual compensating transfer function $H_2(s)$, while $H(s)$ comprises only $H_1(s)$ in sections 3. and 4.

Two $G(s)$s are prepared from the previous results by only using kinesthetic sensation[5]; one is clarified to be the class of the desirable $G(s)$ for a human operator, and the other is one of the hard-to-manipulate classes of $G(s)$.

$$G_1 : (M_D,\, D_D,\, K_D) = (0.56,\, 56,\, 33),$$
$$G_2 : (M_D,\, D_D,\, K_D) = (0.56,\, 56,\, 925),$$

The actual spring in G_1 cannot be prepared, so the computer simulates the virtual spring as the object in this section. Then, the maneuver transfer function

$$G(s) = \frac{s}{M_D s^2 + D_D s + K_D} \frac{1}{Ts+1} \frac{1 - \frac{L}{2}s}{1 + \frac{L}{2}s} \tag{25}$$

is obtained. The parameters of $G_\Delta(s)$ is also arbitrary, so they are chosen as subsection 4.2.

5.2. Experimental results and discussions

Figure 11(a) shows the frequency responses of $G(s)H(s)$s for G_1 with only kinesthetic sensation and both sensations. Similarly, Fig.11(b) shows those for G_2. In addition, Figure 12 compares the frequency responses of $G(s)H(s)$s for G_1 and those for G_2 with both sensations.

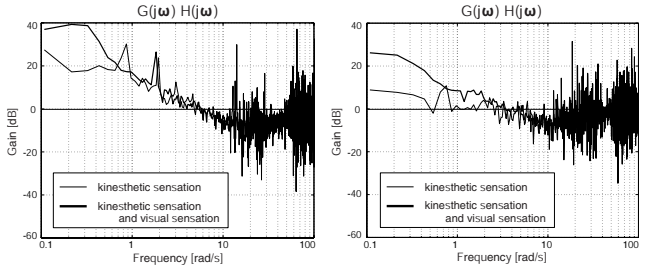

(a) Open-loop frequency responses for G_1.

(b) Open-loop frequency responses for G_2.

Fig. 11. Comparison of open-loop frequency responses only using the kinesthetic sensation (thin line) and those of using both kinesthetic and visual sensations (thick line).

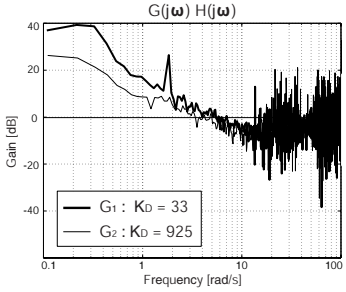

Fig. 12. Comparison of open-loop frequency responses for the two $G(s)s$ with visual sensation: G_1 (thick line) and G_2 (thin line).

1. Figure 11 shows that the operator using both kinesthetic and visual sensations can yield a higher open-loop gain at low frequencies; however, he cannot increase his crossover frequency. Therefore, with both sensations, the subject can operate the machine better in lower frequencies but with almost the same bandwidth.
2. From Fig.12, G_1 yields a higher gain at low frequencies and a higher crossover frequency than G_2. Thus, G_1 is more desirable than G_2 when both sensations are employed, as well as when only kinesthetic sensation is employed.

Although it depends on an operator, the highest crossover frequency only with the kinesthetic sensation is 10[rad/s], and that of the visual sensation is less than 5[rad/s]; the information from the visual sensation is likely to lead results 1 and 2. From result 3, specifying the desirable class of the maneuver transfer function also plays an important role in designing HMCSs using both kinesthetic and visual sensations, similarly as when only the kinesthetic sensation is employed. Moreover, the desirable class is similar.

6. Conclusions

The authors have investigated influences of manipulator dynamics on stability and feasible classes of HMCSs based on two control designs: virtual tool dynamics, focusing on tool dynamics and reaction force transfer function; and our design method, specifying maneuver transfer function and transfer function for object dynamics variation. On the basis of both designs, experiments using an actual spring have been performed, only employing kinesthetic sensation. The other experiments have clarified roles of kinesthetic sensation and visual sensation. Using visual sensation has improved self-shaping characteristics of a subject at low frequencies; however, it cannot affect the crossover frequency. Therefore, our previous design only considering kinesthetic sensation is also valid even when a human operator use his/her eyes in operation and the dynamics of the manipulator are considered.

As future plans, the present control system design considering manipulator dynamics is very simple, so more sophisticated design methods such as H_∞ control should be examined. Besides, further studies on the roles of kinesthetic sensation and visual sensation will be required.

References

[1] H. Kazerooni, Human-Robot Interaction via the Transfer of Power and Information Signals, *IEEE Trans. on Systems, Man and Cybernetics*, Vol.20, No.2, pp.450-463, 1990.

[2] K. Kosuge, Y. Fujisawa, and T. Fukuda, Control of Man-Machine System Based on Virtual Tool Dynamics (in Japanese), *Trans. of the Japan Society of Mechanical Engineers series C*, 60-572, pp.1337-1343, 1994.

[3] T. Inaba and Y. Matsuo, Loop-shaping Characteristics on Hand Position Control of a Human Operator in a Human-Machine Control System (in Japanese), *Trans. IEE of Japan*, 119-C-2, pp.269-275, 1999.

[4] T. Inaba and Y. Matsuo, On Parametrization of Control Systems for Human-Machine Cooperative Systems Stabilizing Their Tool Dynamics and Maneuver Transfer Functions, *SICE2002*, WA12-6, 2002.

[5] T. Inaba and Y. Matsuo, On Control System Design of a Human-Machine Cooperative System Considering Self-shaping Characteristics of its Human Operator and Recognition of Object Dynamics Variation, *CIRA2003*, 2003.